scientific reports

Check for updates

OPEN

Green synthesized CaO decorated ternary CaO/g-C_3N_4/PVA nanocomposite modified glassy carbon electrode for enhanced electrochemical detection of caffeic acid

Annamalai Karthika[1], C. Sudhakar[2], Periyakaruppan Karuppasamy[3]✉, Baluchamy Tamilselvi[4], Subramaniam Meena[3], Kurupalya Shivram Anantharaju[3], K. B. Tan[5]✉ & H. C. Ananda Murthy[6,7]✉

A highly selective, sensitive caffeic acid (CA) detection based on calcium oxide nanoparticles (CaO NPs) derived from extract of *Moringa oleifera* leaves decorated graphitic carbon nitride covalently grafted poly vinyl alcohol (CaO/g-C_3N_4/PVA) nanocomposite modified glassy carbon electrode (GCE) was studied. A facile sonochemical method was adapted to synthesis nanomaterials and characterized by HR-TEM (High resolution transmission electron microscopy), FT-IR (Fourier transform infrared spectroscopy), XRD (X-ray diffraction), FE-SEM (Field emission scanning electron microscopy), EDX (Energy dispersive X-ray analysis), Mapping and BET (Brunauer-Emmett-Teller) analysis, and electrochemical techniques. The nanocomposite modified GCE exhibited an excellent catalytic performance to the oxidation of CA under optimized conditions owing to better electron transfer efficiency, conductivity and high surface area of the electrode material. The present electrochemical sensor showed high selectivity towards the determination of 10 µM CA in the presence of 100-fold higher concentrations of interferents. The modified CA sensor exhibited a wide sensing linear range from 0.01 µM to 70 µM and the detection limit (LOD) was found to be 0.0024 µM (S/*N* = 3) in 0.1 M phosphate buffer saline (PBS) as a supporting electrolyte at pH 7.0. The fabricated CA sensor provides an excellent stability, reproducibility and selectivity for the determination of CA. The modified CA sensor was applied to real blood plasma samples and obtained good recovery (97.6-100.1%) results.

Keywords Caffeic acid (CA), Anticancer drug, Electrochemical Sensor, CaO/g-C_3N_4/PVA nanocomposite, Plasma samples, Amperometric study

Caffeic acid (CA) possessed a phenylpropanoid assembly and 3,4-dihydroxylated aromatic rings fused with carboxylic acid via *trans* ethylenic bond. CA is acting an ergogenic, antioxidant, diuresis, and stimulating agent for the human central nerve systems. CA is the compound has various functionality which is used up extensively beverages such as chocolate, coffee beans, energy boost drinks and tea leaves[1]. CA is also consumed in pharmaceutical designs for the neurodegenerative disorders in human body. Caffeic acid (CA) existing in

[1]Department of Chemistry, Thiagarajar College, Madurai 625 009, Tamilnadu, India. [2]Department of Chemistry, K.P. National College of Arts and Science, Batlagundu 624202, India. [3]Department of Chemistry, Dayananda Sagar College of Engineering, Bangalore 560111, Karnataka, India. [4]Department of Chemistry, K.L.N. College of Engineering, Pottapalayam 630612, Tamilnadu, India. [5]Department of Chemistry, Faculty of Science, Universiti Putra Malaysia, Serdang 43400, Selangor, Malaysia. [6]School of Applied Sciences, Papua New Guinea University of Technology, Lae 411, Morobe Province, Papua New Guinea, Papua New Guinea. [7]Department of Prosthodontics, Saveetha Institute of Medical and Technical Science (SIMATS), Saveetha Dental College & Hospital, Saveetha University, Chennai 600077, Tamil Nadu, India. ✉email: periyakaruppankaruppasamy@gmail.com; tankarban@upm.edu.my; anandkps350@gmail.com

numerous food products and plants as an essential hydroxycinnamic acid and it provides an antibacterial, anti-inflammatory, antineoplastic and antioxidant properties to the human body. Meanwhile, overconsumption of CA leads negative impact to the human health. Hence, quantitative determination of CA in foods and pharmaceuticals are much essential and needs to be estimated accurately using highly sensitive, low-cost devices now a day[2]. Various analytical techniques such as capillary electrophoresis-mass spectrometry (CE-MS)[3], GC-MS (gas chromatography coupled mass spectrometry)[4], high-performance liquid chromatography (HPLC)[5,6], LC-MS (liquid chromatography coupled mass spectrometry)[7], capillary gas chromatography (CGC), electron-spray ionization mass spectroscopy (ESI-MS)[8], electrophoresis-mass spectrophotometry[9], spectrophotometry[10,11], colorimetric[12], photoelectrochemical[13], and Electrochemical[14–21] techniques were utilized for the detection of CA at different ranges of concentrations. Among the aforementioned techniques, electrochemical techniques are one of the accurate techniques and it has received more attention for the highly selective and sensitive determination of biological, environmental and pharmaceutical real time analysis due to their high selectivity, ease response, cost effective, facile maneuver, portability, good sensitivity and less chemical wastage respectively[22–24]. However, the detection of CA using conventional bare working electrode is not so easy owing to its deprived electrochemical replies. Recently, electrochemical detection of CA using modified working electrodes is receiving much attention due to their excellent catalytic properties towards CA[25,26]. From a series of literatures, the use of graphene carbon nitride (g-C_3N_4) and its hybrids has been acclaimed in the modification of electrodes for improving the detection limits as well as detection ranges of the analytes[27–29]. Moreover, the structural insights of g-C_3N_4 can be changed at any cost via doping the external materials on the layered structure of g-C_3N_4[30]. Modification of working electrodes via non-enzymatic approach utilized various NPs such as CNTs, metal-organic frameworks (MOFs), graphene/reduces graphene oxides (GO/rGO) and metal oxides (MOs) are an important[14,31–34].

Among the aforementioned NPs, metal oxides NPs are one of the important potential nanomaterials used as electrode material for the modification of working electrodes due to its non-toxic nature, higher surface to volume ratio, good stability, better conductivity, and faster response, excellent catalytic property[36]. As per the reported literatures, calcium oxide (CaO) nanomaterial is not reported for CA sensing using electrochemical techniques. Many chemical methods have been employed to synthesis CaO NPs such as microwave-assisted, solution combustion, sol-gel, surfactant assisted and thermal decomposition methods[34–37]. In addition, the abovementioned synthesis methods, lots of chemicals are involving, and create pollution to the environment. However, to synthesize of CaO NPs by greener way is receiving much attention now a day and minimal reported literatures are available[38]. CaO nano metal oxides have been utilized for modification of electrode material for CA sensing applications using electrochemical techniques due to its idiosyncratic electrical and catalytic properties. A feasible way to enhance the sensing performance is doping the metal oxides over the 2D-layered g-C_3N_4-based materials which enhance the sensitivity and selectivity, catalytic property, reduces the operating temperature, response and recovering time respectively. Recently, it is in vogue that the sensitivity and selectivity of the electrode materials are boosted by doping metal oxides with conducting polymers. Among the conducting polymers, polyvinyl alcohol (PVA) is an important and it has wide-spectrum of applications due to its cost-effective nature, corrosion resistance, non-toxicity, good conductivity, ease blending nature with other materials, and rapid redox behavior. Numerous materials were utilized for CA monitoring studies such as metal nanoparticles (MNPs), Metal oxides (MOs), metal hydroxides (MOHs) used for CA detection have been studied and improved, such as carbon nanomaterials, and conducting polymers (CPs). Recent studies are focusing the combination of CPs (PE, PVA, & PEPOT), MNPs (Au, Pt, Pd, & V) and carbon materials (CNTs, MWCNTs, rGO & graphene). The aforementioned material combinations allowed novel properties to the electrochemical sensors owing to larger surface area, excellent functionality, hydrophobic property, biocompatibility and synergistic effect[38]. Recently, ternary bio-metal oxides-based nanomaterials are receiving great attention in the electrocatalysis field owing to their simple preparation, less toxicity, various oxidation states, cost-effectiveness, eco-friendly nature, natural richness and wide range of applications. For instances, PVA grafted G-C_3N_4 with V_2O_5 nanomaterial has used for the detection of folic acid by electrochemical sensing techniques[38]. Erady and co-workers investigated CA sensing based on carbon paste electrode (CPE) surface modified using bismuth (Bi), multi-layered carbon nanotubes (MCNTs) and cetyltrimethylammonium bromide as a supporting electrolyte by differential pulse voltammetry technique at various pH and scan rates. The electrochemical response was found to be linear ranges between 6.0×10^{-8} M and 5.0×10^{-4} M and LOD was estimated to be 0.157 nM ($S/N=3$). The detection of CA in real samples (fruit juices, tea & coconut water) were provided excellent results[39]. Botelho et al. studied the detection of CA based on a novel photoelectrochemical sensor developed using titanium dioxide (TiO_2) NPs, CNTs, and cadmium telluride quantum dots (CdTeQDs). The photochemical sensor exhibited a wide linear response range between 0.5 µM and 360 µM with a LOD value of 0.15 µM. The developed sensor utilized for the detection of CA in real samples such as Tea and coffee samples and the recovery result were found to be 99.9 & 97.4 percentages[40]. Nehru et al. synthesized f-MWCNTs/-$NaFeO_2$ nanocomposite by ultrasonication method and used as sensing material for the detection of CA. The fabricated electrochemical sensor exhibited ultra-sensitivity value of 44.685 $\mu A.\mu M^{-1}cm^{-2}$, excellent linearity and a LOD value of 0.002 µM while using DPV technique[41]. Sakthivel et al. prepared $CoFeSe_2$ functionalized carbon nanofibers (f-CNF) by hydrothermal method and the composite material coated on the surface of glassy carbon (GC) electrode. The composite modified GC electrode utilized for the detection of CA and the LOD value was found to be very low (0.002 pM) and the sensitivity was evaluated to be 2.04 $\mu M^{-1}cm^{-2}$ using differential pulse voltammetry technique[42]. Thangavelu et al. reported the determination of CA using reduced Graphene Oxide (rGO)/Polydopamine (PDA) composite modified electrode by differential pulse voltammetry method. The response range was observed to be linear (5.0 nM − 450.55 µM) and the LOD value was calculated to be 1.2 nM. The modified electrode exhibited an acceptable selectivity in the presence of excess concentrations of other interferents and applied to the real time wine samples and obtained good recovery results[33].

This work aims to synthesis CaO/g-C_3N_4/PVA nanocomposite material using sonochemical method and fabricate CaO/g-C_3N_4/PVA nanocomposite modified glassy carbon electrode (CaO/g-C_3N_4/PVA/GCE). The as-synthesized materials are well characterized by various spectral, analytical, electrochemical techniques. The modified CA sensor was utilized for the accurate determination of CA in 0.1 M PBS at pH 7.0 using electrochemical techniques such as CV and amperometric techniques. The practicability of the CA sensor was tested using real time blood plasma samples. This work paves a way that the present modified sensor may be used for an accurate determination of CA in food and health-care products.

Experimental section

Materials

Analytical grade (AR) chemicals such as Ascorbic Acid (AA), Caffeic acid (CA), Catechin (CT), Catechol (CC), Chlorogenic acid (CGA), Dopamine (DA), Epinephrine (EP), Hydroquinone (HQ), Gallic acid (GC), Epicatechin (EC), Poly vinyl alcohol (PVA), Potassium chloride (KCl), Thiourea, NaOH, and Uric Acid (UA) were purchased from sigma-Aldrich with 99.9% purity, India and used as such. Phosphate buffer (PB) solution was prepared by mixing molar volume ratios of monosodium dihydrogen phosphate (NaH_2PO_4, 0.5 M) and disodium monohydrogen phosphate (Na_2HPO_4, 0.5 M) solutions[25]. *Moringa oleifera leaves* were collected from inside the campus of Thiagarajar College, Madurai-625 009, Tamilnadu, India. Blood plasma samples were collected from the Government Rajaji Hospital, Madurai, India. All the required solutions were prepared using deionized water (DI) water. A mirror like polished glassy carbon electrode was used as a working electrode, Pt-wire utilized as a counter electrode and $Ag/AgCl_{(sat.KCl)}$ utilized as a reference electrode for entire electrochemical studies.

Synthesis of CaO NPs from *Moringa oleifera* leaves

The *Moringa oleifera* leaves cast-off stems and stalks were washed with DD water and dried at sunlight for 7 days. Dried leaves were powdered using mixer grinder and the powdered *Moringa oleifera* (5 g) dispersed in DI water and boiled at 50 °C for 45 min. Colour of the *Moringa oleifera* extract was changed into brown then filtered and cooled. The filtrate was stirred using bath ultrasonicator and 5 g of anhydrous calcium nitrate was added for maintaining basic condition of the extract solution by adding little drops of 1 M NaOH solution and boiled at 60 °C till it changed into yellow paste[43]. Subsequently, the solution was filtered by Whatman filter paper with funnel. The filtered precipitate was transferred into silica crucible and kept inside the muffle furnace for 1 h at 450 °C. Finally, a white coloured CaO NPs powder was obtained[37].

Synthesis of CaO/PVA and g-C3N4

To synthesis CaO/PVA nanomaterial, 0.3 g of PVA and 3 g of CaO (1:10 v/v ratio) were dispersed in 50 mL of DI water followed by ultrasonication in 300 W for 2 h[38]. Then the mixture was stirred and heated at 60 °C for 30 min and the obtained precipitate was eviscerated with ethanol and DI water for several times. The precipitate was dried in hot-air oven at 80 °C for 8 h. Further, it was calcined in muffle furnace at 300 °C for 1 h and dried. To synthesize g-C_3N_4, 6 g of thiourea was calcinated ~ 450 °C by silica crucible in a programmable muffle furnace for 2 h as per the literature[27,30]. The colour of the product was changed into pale yellow. The pale-yellow powder g-C_3N_4 (4 g) was dispersed into 100 mL of 0.1 M NaOH and ultrasonicated (3000 rpm) for 3 h. The obtained reaction mixture was poured into Teflon bomb and closed by stainless steel and kept inside the hydrothermal oven for 3 h at 150 °C. Finally, dried pale-yellow colour activated g-C_3N_4 nano-layered material was obtained and purified using DI water and dried in a hot air oven at 80 °C for 1 h.

Synthesis of ternary CaO/g-C3N4/PVA nanocomposite

CaO/PVA and g-C_3N_4 with the propositions (1:10 v/v ratio) of 0.2 M (1.18 mg in 30.0 mL) and 2 M (~ 10.1 mg in 30.0 mL) were dispersed in 50.0 mL beaker. The reaction mixture was ultrasonicated for 2 h and then the resultant pale orange product collected by centrifugation. Centrifuged product was washed using deionized water and dried at 90 °C for 8 h in a hot air oven is shown in Fig. 1.

Fabrication of ternary CaO/g-C3N4/PVA modified glassy carbon electrode

GCE was well polished with 0.3 and 0.05 µm alumina slurries on velvet cloth following eight-shaped cleaning technique and sonicated in deionized water for removing impurities. Mirror-like polished GCEs used for the fabrication of electrochemical sensor. The as-synthesized CaO/g-C_3N_4/PVA (2.0 mg/mL) was ultrasonicated in ethanol and drop-casted about 6.0 µL of mixtures on pre-treated GCE using micro-syringe and dried at room temperature.

Characterization techniques

XRD (XPERT-3 diffractometer with Cu Kα radiation (K = 1.54 Å)) to analyze the crystalline properties. Fourier Transform Infra-Red (FT-IR) spectrum was recorded in JASCO FT/IR-6600 instrument. HRTEM (JEOL 2100 F) instrument was used to study the structural characteristics. Hitachi S-3000 H Scanning Electron Microscopy (SEM) instrument was used to analyze surface morphology. Energy dispersive X-ray (EDX) spectrum was recorded using HORIBA EMAX X-ACT with Hitachi S-3000 H scanning electron microscope. Quantachrome instrument – 5.0 version with N_2 adsorption-desorption at 80 ± 0.5 K for 10 h in vacuum condition used for BET analysis. The electrochemical behavior (cyclic voltammetry (CV) & electrochemical impedance spectroscopy (EIS)) of the nanomaterials modified GCE was examined using CHI-611 A and amperometry was run in CHI-900 electrochemical analyzers.

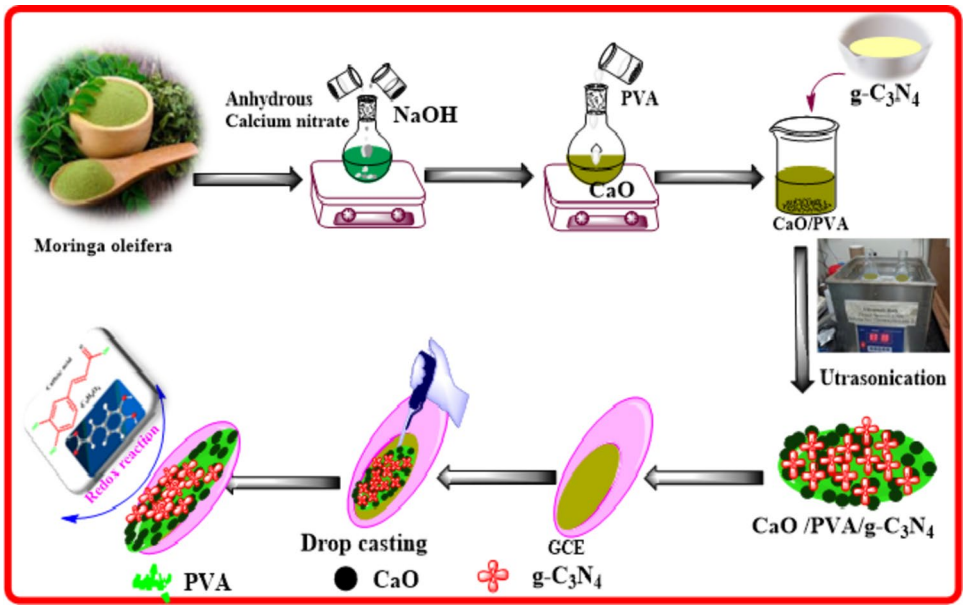

Fig. 1. Synthesis routes of CaO/g-C_3N_4/PVA nanocomposite.

Results and discussion

Powder XRD and FTIR analysis

The crystalline nature of (a) CaO, (b) CaO/PVA, (c) CaO/g-C_3N_4 and CaO/g-C_3N_4/PVA was analyzed by PXRD and the obtained results are shown in Fig. 2A. Figure 2A (a) exhibits the distinctive characteristic peaks at 23.18°, 29.54°, 36.14°, 39.14°,43.28°, 47.2°, 47.68°, 48.68°, 56.16°, 56.94°, 57.58°, 59.54°, 61.08°, 63.34° (JCPDS card no. 00-004-0777) corresponding to CaO (hkl) planes[37]. XRD peak for PVA reinforced CaO NPs were shifted towards low 2θ value side increasing the crystallinity of CaO/PVA nanocomposite as illustrated in Fig. 2A (b). After the addition of g-C_3N_4 with CaO NPs a new peak was obtained at 2θ = 28.3 owing to the amorphous nature of pure g-C_3N_4 as displayed in Fig. 2A (c) (JCPDS card no. 87-1526)[30]. Moreover, XRD peaks of CaO, g-C_3N_4 and PVA appear in the XRD pattern of CaO/g-C_3N_4/PVA composites as exposed in Fig. 2A (d) (JCPDS card no. 00-037-1497), signifying that the three component peaks are hybridized successfully[1]. XRD result confirms that the PVA and g-C_3N_4 was assimilated with CaO NPs and the average particle size was calculated between 20 nm and 30 nm. CaO/g-C_3N_4/PVA nanocomposite material was exhibited all the three components hybridized XRD peaks with significant enhancement of intensity as compared to the XRD peak intensities of a) CaO, (b) CaO/PVA, (c) CaO/g-C_3N_4 materials[38].

Figure 2B displays that the FTIR spectra for a) CaO, (b) CaO/PVA, (c) CaO/g-C_3N_4 and CaO/g-C_3N_4/PVA. For pure CaO, FTIR peak was detected at 1642 cm^{-1} which corresponds to O-H bending/stretching vibrations. FTIR peaks at 1459 cm^{-1}, 713 cm^{-1}, and at 877 cm^{-1} were ascribed to asymmetric stretching, out-of-plane and in-plane bending vibrations of CO_3^{2-} ions[22]. In addition, PVA described the peaks at 2927 cm^{-1} and 2854 cm^{-1} for the presence of symmetric and asymmetric -CH_2 stretching vibrations. Symmetric stretching of carboxylate anion –COO^- provided the FTIR peak at 1641 cm^{-1}. Figure 2B (c) and (d) (CaO/g-C_3N_4 and CaO/g-C_3N_4/PVA) the peaks between 3305 and 3000 cm^{-1} were ascribed to stretching vibration modes of N-H bonds resulting from the incomplete condensation of amino groups. Peaks appeared at 889 cm^{-1} and 806 cm^{-1} were attributed to vibration mode of tri-s-triazine and the twist mode of N-H bonds respectively. The FTIR peaks were observed the ranges between 1700 and 1200 cm^{-1} indicating the characteristic stretching frequencies of C-N bonds.

Electrochemical and BET analysis

Figure 2C shows the CV response for bare GCE (a), CaO (b), CaO/PVA (c), CaO/g-C_3N_4 (d) and CaO/g-C_3N_4/PVA modified GCE (e) in 0.1 M PBS in the absence of CA and Fig. 2D shows the CV response for bare GCE (a), CaO (b), CaO/PVA (c), CaO/g-C_3N_4 (d) and CaO/g-C_3N_4/PVA modified GCE (e) in 0.1 M PBS in the presence of 10 µM CA containing at a scan rate of 50 mV/s. There was no redox peak for CA in bare GCE as shown in Fig. 2C (a) & Fig. 2D (a). However, discreet redox peaks were obtained for CaO, CaO/PVA and CaO/g-C_3N_4 modified GCEs in the presence of CA as compared to CV responses of the modified electrodes in the absence of CA in 0.1 M PBS at a scan rate of 50 mV/s owing to the lower electrochemical response of CA as given in curves (b-d). In contrast, CaO/g-C_3N_4/PVA modified GCE (e) exhibited a distinct redox peak for 10 µM CA owing to higher surface area and electron transfer (ET) nature of the electrode material compared to CaO/g-C_3N_4/PVA modified GCE in the absence of CA is depicted in Fig. 2C (e) & Fig. 2D (e). In addition, ternary CaO/g-C_3N_4/PVA nanocomposite showed a strong synergistic effect owing to an inter-component interaction among CaO, g-C_3N_4, and PVA which enhances the rate of ET and electrocatalytic process. EIS is an important technique to examine the interface properties like electron transfer resistance (Ret) for bare GCE, CaO/PVA, CaO/g-C_3N_4 and CaO/g-C_3N_4/PVA modified GCEs in 0.1 M PBS at pH 7.0 is shown in Fig. 2E. EIS semicircle

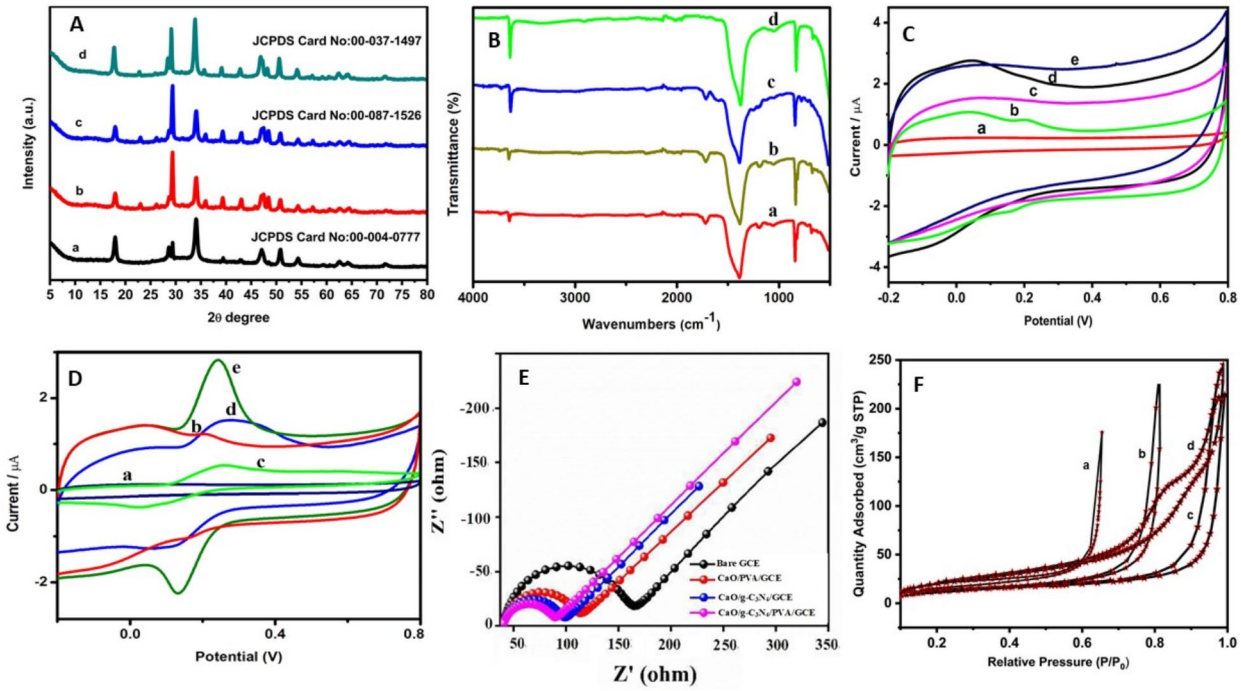

Fig. 2. (**A**) XRD spectra. (**B**) FT-IR spectra of (a) CaO, (b) CaO/PVA, (c) CaO/g-C_3N_4 and (d) CaO/g-C_3N_4/PVA nanomaterials. (**C**) CV responses of (a) Bare GCE (b) CaO/GCE (c) CaO/PVA/GCE (d) CaO/g-C_3N_4/GCE and (e) CaO/g-C_3N_4/PVA/GCE in the absence of CA in 0.1 M PBS at scan rate of 50 mV/s. (**D**) CV responses of (a) Bare GCE (b) CaO/GCE (c) CaO/PVA/GCE (d) CaO/g-C_3N_4/GCE and (e) CaO/g-C_3N_4/PVA/GCE in the presence of 10 μM CA in 0.1 M PBS at scan rate of 50 mV/s. (**E**) EIS spectra of Bare GCE, CaO/PVA/GCE, CaO/g-C_3N_4/GCE and CaO/g-C_3N_4/PVA/GCE modified electrodes. (**F**) BET (N_2 adsorption-desorption) curves of (a) CaO, (b) CaO/PVA, (c) CaO/g-C_3N_4 and (d) CaO/g-C_3N_4/PVA nanomaterials.

provides the information about electron transfer resistance of the electrode material. CaO/g-C_3N_4/PVA showed the smaller semicircle compared to other nanomaterials owing to a fast electron transfer process at interface[31]. However, bare GCE exhibited larger semicircle as compared to CaO/PVA, CaO/g-C_3N_4 to CaO/g-C_3N_4/PVA modified GCEs due to inhibitive electron transfer process at the interface[30,31]. The Ret values were decreased while increasing the EIS semicircle diameters and the Ret values were evaluated between 3.72 Ωι cm^2 and 0.85 Ωι cm^2 for bare GCE, CaO/PVA, CaO/g-C_3N_4 to CaO/g-C_3N_4/PVA modified GCEs.

The distribution of pore size and adsorption-desorption of N_2 for (a) CaO, (b) CaO/PVA, (c) CaO/g-C_3N_4 and (d) CaO/g-C_3N_4/PVA were analyzed by Brunauer-Emmett-Teller (BET) is depicted in Fig. 2F. The BET results show that the adsorption-desorption isotherm was categorized into type IV indicating the disordered meso-/microspores structure of CaO/g-C_3N_4/PVA and hysteresis loops were categorized as H3. It was observed that the high adsorption capacity and relative pressure (P/P_0) about greater than 0.6 for all the nanomaterials[44]. The pore volume of CaO/g-C_3N_4/PVA was found to be 0.165 cm^3/g. The specific surface area of CaO/g-C_3N_4/PVA was calculated to be 18.56 m^2/g and the pore diameter assessed to be 30 nm using the Barret-Joyner-Halenda (BJH) method which is higher value compared to CaO, CaO/PVA, and CaO/g-C_3N_4 respectively. The higher value of specific surface area indicates the agglomeration of CaO NPs which is good agreement with the HR-TEM data. The increased surface area and pore volume distribution of CaO/g-C_3N_4/PVA enhances the electrocatalytic redox process of CA[45].

SEM and EDX analysis

The size and morphology of (a) CaO, (b) CaO/PVA, (c) CaO/g-C_3N_4 and (d) CaO/g-C_3N_4/PVA is shown in Fig. 3. FE-SEM image of CaO clearly shows the nanosheets (Fig. 3 (a)). Figure 3(b) and (c) exhibit the characteristic FE-SEM images of CaO/PVA (agglomerated rice-rod shape), and CaO/g-C_3N_4 (randomly distributed nanorods). But Fig. 3(d) & (e) indicates the formation of agglomerated rods like nano-cone structure for CaO/g-C_3N_4/PVA. Figure 3(f) shows the EDX spectrum of CaO/g-C_3N_4/PVA, which confirms the presence of Ca, O, C, and N elements. The percentage of composition of elements such as Ca, O, C, and N are tabulated and given in Table S1. The colored elemental mapping images in Fig. 3(g-k) show the Ca (red), N (green), O (blue) and C (yellow) elements. Bar diagram for SEM-EDX analysis of CaO/g-C_3N_4/PVA nanocomposite is given in Fig. 3(l).

HR-TEM and SAED analysis

HR-TEM is used to find the morphology, phase and crystallographic evidence for the materials. The meso-porous hexagonal structure of CaO NPs was agglomerated to form larger size hexagonal shape particles and

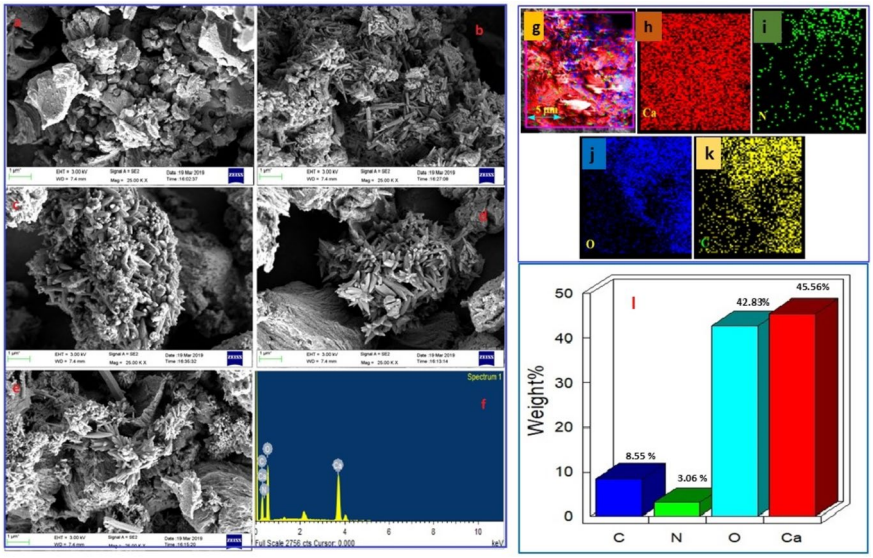

Fig. 3. FE-SEM image of (**a**) CaO, (**b**) CaO/PVA, (**c**) CaO/g-C_3N_4, (**d**, **e**) CaO/g-C_3N_4/PVA nanomaterials and (**f**) EDX spectrum of CaO/g-C_3N_4/PVA nanocomposite. (**g**-**k**) Mapping of elements of CaO/g-C_3N_4/PVA nanocomposite. (**l**) SEM-EDX analysis of percentage of elements present in CaO/g-C_3N_4/PVA nanocomposite.

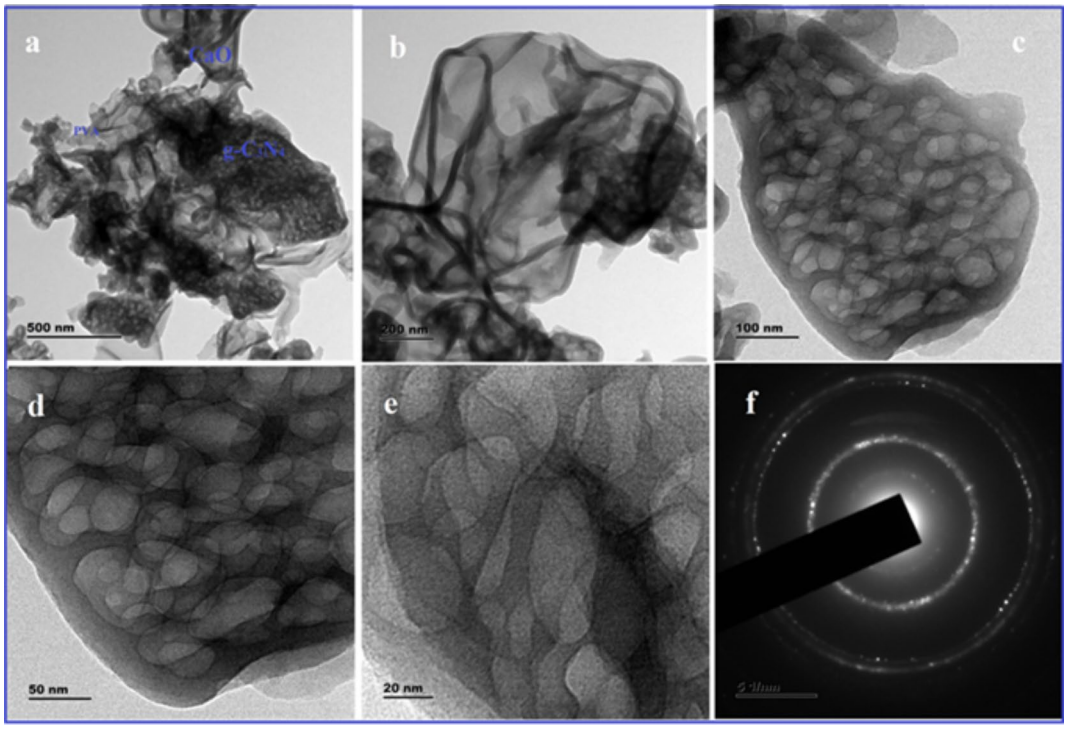

Fig. 4. HR-TEM image of (**a**-**e**) CaO/g-C_3N_4/PVA and (**f**) SAED pattern of CaO/g-C_3N_4/PVA nanocomposite.

the particle size was found to be less than 30 nm. When the covalently grafted PVA on the exterior of g-C_3N_4 layered structure blend with CaO NPs, the thickness of the hexagonal shape was increased which attributes that the homogenous distribution with CaO NPs. The hexagonal morphology of the CaO/g-C_3N_4/PVA material's particle size was found to be less than 30 nm which is inaccordence with the average crystallite size calculated by XRD. HRTEM results were comparable with reported values of other ternary composite material[37,46]. HR-TEM images are depicted in Fig. 4(a-d) showed that the hexagonal shape owing to the linking of huge size particles of CaO and nanosheets of g-C_3N_4 on PVA surface. CaO/g-C_3N_4/PVA displays the hexagonal like structure and an increased thickness was attributed to the covalently grafting of PVA on the exterior of g-C_3N_4. Figure 4(e)

indicated the crystal-like structure of CaO/g-C_3N_4/PVA in the selected area of the electron diffraction (SAED pattern as given in Fig. 4(f)).

Impact of concentration, pH, and sweep rate

CaO/g-C_3N_4/PVA modified GCE was utilized to analyze the electrochemical performance while changing CA concentration between 10 µM and 150 µM in 0.1 M of PBS (pH 7.0) at scan rate of 50 mV/s is shown in Fig. 5. It can be seen that the CA redox peak increased while increasing CA concentration from 10 µM to 150 µM and the anodic peak current was increased with trivial anodic potential shift as shown in Fig. 5(a). The plot of CA concentration against current is depicted in Fig. 5(b) and it exhibits a linear relationship (Ipa = 0.0161x + 0.82) with correlation coefficient (R^2) value of 0.9944 supports the catalytic efficiency of CaO/g-C_3N_4/PVA modified GCE towards CA. Impact of pH on the CV response of CA was examined in PBS between pH 3.0 and pH 9.0 containing 10 µM of CA at a scan rate of 50 mV/s are shown in Fig. 5(c) which indicates that the anodic peak current (Ipa) of CA at CaO/g-C_3N_4/PVA modified GCE is pH dependent. The anodic peak potential shifts to more positive potential values with an increase in pH and the separation between the anodic and cathodic peak potentials increased. The plot of pH against oxidation peak potential indicated that the peak potential was increased while increasing the pH value from 3.0 to 7.0 but it was decreased above 7.0 is shown in Fig. 5(d). In addition, higher peak current was observed at pH 7.0 for revisable redox process of CA which involves two electrons and two protons directly. A large separation of peak potential was found above the pH 7.0 which suggests the sluggish heterogeneous electron transfer reaction between electrode surface and analyte. The slope was found to be higher than 59 mV indicating that the reaction involves more than one electron transfer in CA oxidation. The positive slope and R^2 values suggest that the electron transfer followed by protonation transfer as per the Nernstian systems[47].

Impact of scan rate on the oxidation of CA at CaO/g-C_3N_4/PVA modified GCE with different scan rates (10 − 90 mV/s) in 0.1 M PB solution (pH 7.0) containing 10 µM of CA was analyzed by CV technique are presented in Fig. 5 (e). CV results revealed the anodic peak current increased while increasing scan rate from 10 to 90 mV/s with slight anodic potential shift. ET reaction occurred at the interface between electrode surface and solution at applied potential was found to be linear with respect to the rate of the redox reaction[21]. Excellent linear relationship was attained between different scan rates and anodic peak current which forms a linear regression equation of Ipa = 0.0377 (mV/s) + 0.1225 with a correlation co-efficient of $R^2 = 0.9967$ (Fig. 5 (f)) supports an adsorption-controlled process[21].

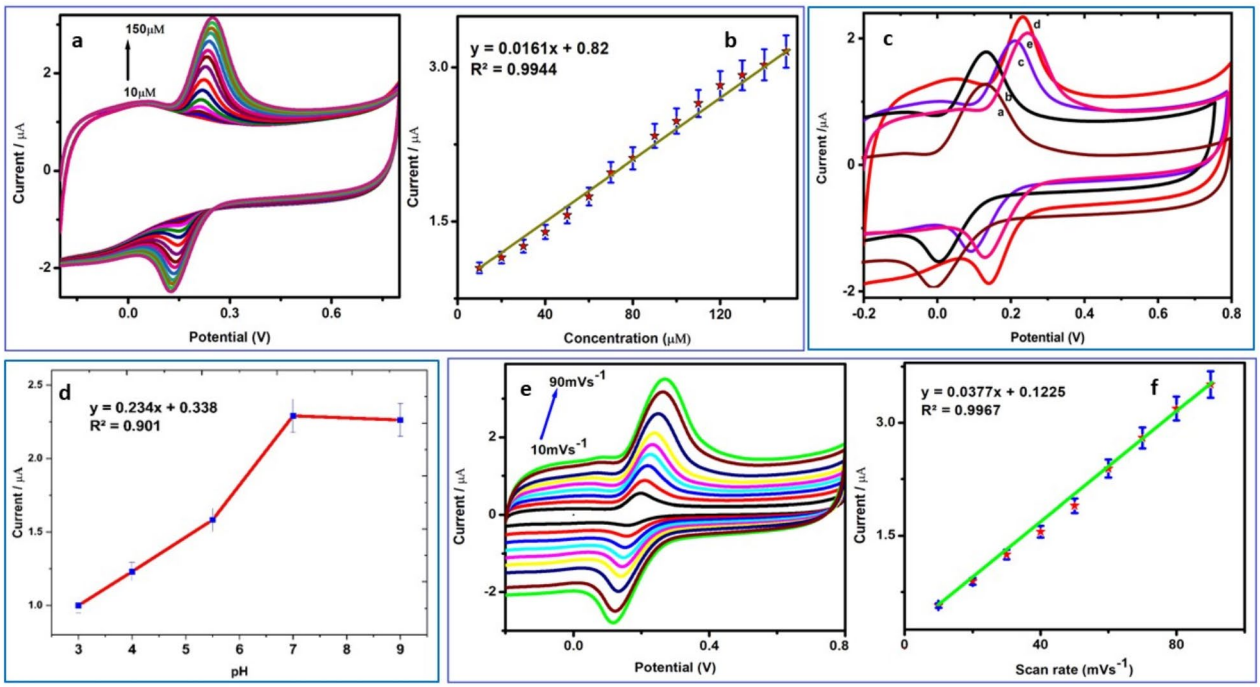

Fig. 5. (**a**) CV responses for CaO/g-C_3N_4/PVA modified GCE in the presence of 10–150 µM of CA and (**b**) Calibration plot of current response vs. concentration of CA. (**c**) CV responses of CaO/g-C_3N_4/PVA modified GCE in 10 µM of CA at different pH values (3.0–9.0). (**d**) Calibration plot of pH vs. Peak Current (µA). (**e**) CV responses of CaO/g-C_3N_4/PVA modified GCE in 10 µM of CA at different scan rates from 10 to 90 mV/s. (**f**) Linear plot for cathodic peak current vs. scan rate.

Effect of loading concentration, interference and mechanistic study

The effect of loading concentration of CaO/g-C_3N_4/PVA nanocomposite on GCE affected cyclic voltammetric response in 10 µM of CA in 0.1 M PBS as a supporting electrolyte at pH 7.0 and the obtained cyclic voltammograms are shown in Fig. 6 (a). The peak current intensity was increased while increasing the volume of CaO/g-C_3N_4/PVA nanocomposite on GCE from 6.0 µL to 10.0 µL. The plot of peak current vs. various volume of the nanocomposite was found to be a linear regression equation of y = 0.694x -3.824 with a correlation co-efficient of $R^2 = 0.9690$ (Fig. 6 (b)).

Interference study for 10 µM of CA with 100-fold excess concentration of various interferents Catechin (CT), Ascorbic Acid (AA), Catechol (CC), Chlorogenic acid (CGA), Dopamine (DA), Epinephrine (EP), Hydroquinone (HQ), Gallic acid (GC), Chlorine (Cl), Copper (Cu) and Sodium (Na) ions in 0.1 M PBS (pH 7.0) as a supporting electrolyte at CaO/g-C_3N_4/PVA modified GCE using amperometric technique is depicted in Fig. 6(c). The observed amperometric results vindicate that the selective detection of CA was achieved at CaO/g-C_3N_4/PVA modified GCE even in the presence of 100-fold higher concentration of various interferents. The fabricated electrochemical sensor showed excellent selectivity towards CA owing to specific electrostatic interface/strong interaction between the hetero atoms of CA molecules and active sites of CaO/g-C_3N_4/PVA electrode surface.

The electrochemical redox reactions of CA at CaO/g-C_3N_4/PVA modified GCE; Oxidation of CA into ortho-quinone derivative ((2E)-3-(3,4–12 dioxocyclohexa-1,5-dienyl) acrylic acid) at + 0.245 V and reduction of ortho-quinone derivative into CA at + 0.186 V occurred efficiently via 2-electron and 2-proton transfer process (Fig. 6 (d)). The electrochemical mechanism for the detection of CA exhibited reversible redox process, first CA oxidized into ortho-quinone derivative ((E)-3-(3,4-dioxocyclohexa-1,5-dien-1-yl) acrylic acid) and then ortho-quinone derivative reduced to CA via reversible process was confirmed CV study[34]. A redox process was observed for CA detection at the surface of the working electrode which corresponds to the reversible redox process involving the transfer of two electrons and two protons[36].

Amperometry detection of CA

Amperometric study was carried out using CaO/g-C_3N_4/PVA modified rotating disk glassy carbon electrode (RDGCE) towards sensing of CA with constant addition of 10 µM of CA ranges between 0.01 µM and 70.0 µM in 0.1 M PBS (pH 7.0) at applied potential of + 0.65 V by means of 1200 rpm rotation speed of the disk. A distinct sharp response was obtained due to addition of CA step by step persistently stirred with 0.1 M PBS (pH 7.0) and the steady state current (SSC) was reached about 3 s indicating the fast response characteristics of the CaO/g-C_3N_4/PVA modified RDGCE sensor. At optimum condition, the obtained amperometry results at CaO/g-C_3N_4/PVA modified RDGCE for CA detection is depicted in Fig. 7 (a). A well-defined sharp amperometric current response was observed for each addition of CA owing to quick electrochemical response of CA at CaO/g-C_3N_4/

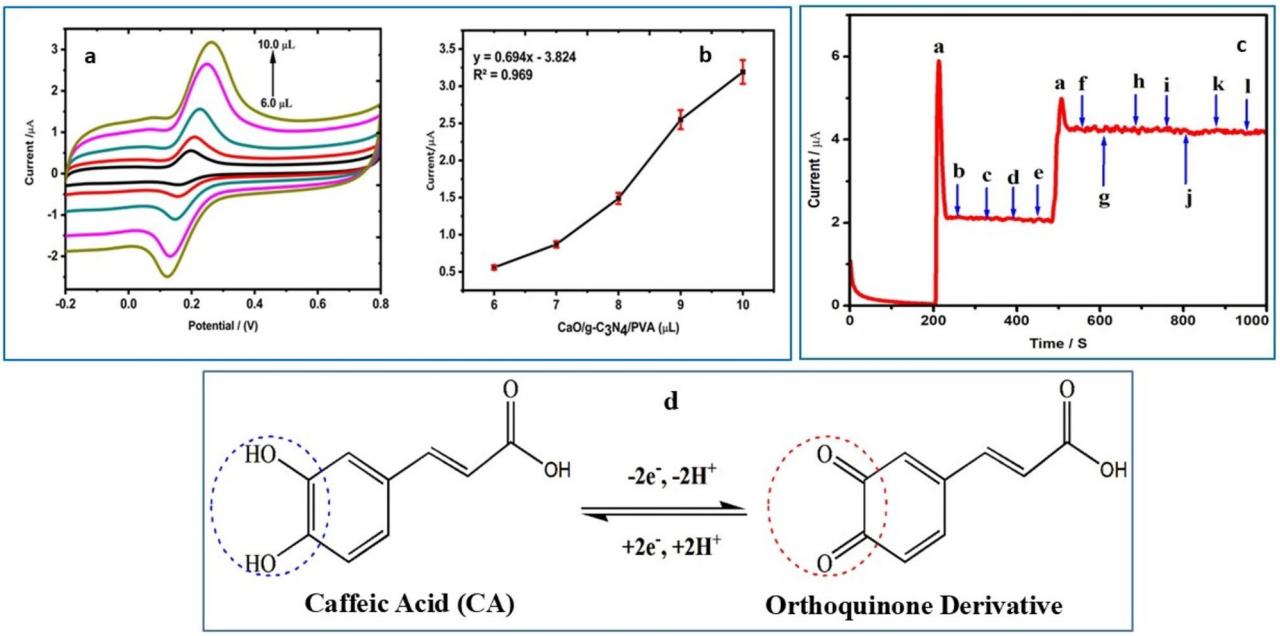

Fig. 6. (**a**) CV responses for the loading concentration of CaO/g-C_3N_4/PVA nanocomposite modified GCE in the presence of 10µM CA and (**b**) Calibration plot of current response vs. volume of CaO/g-C_3N_4/PVA nanocomposite. (**c**) Amperometry response for CaO/g-C_3N_4/PVA modified GCE to successive addition of 0.1 µM CA (a) in the presence of 100-fold excess of concentrations of CT (b), AA (c), CC (d), CGA (e), DA (f), EP (g), HQ (h), GC (i), Cl^- (j), Cu^+ (k) and Na^+ (l) in 0.1 M PBS (pH 7.0) as a supporting electrolyte at a potential of + 0.85 V. (**d**) Mechanism of reversible redox processes (oxido-reduction) of CA at CaO/g-C_3N_4/PVA modified GCE in 0.1 M PBS (pH 7.0).

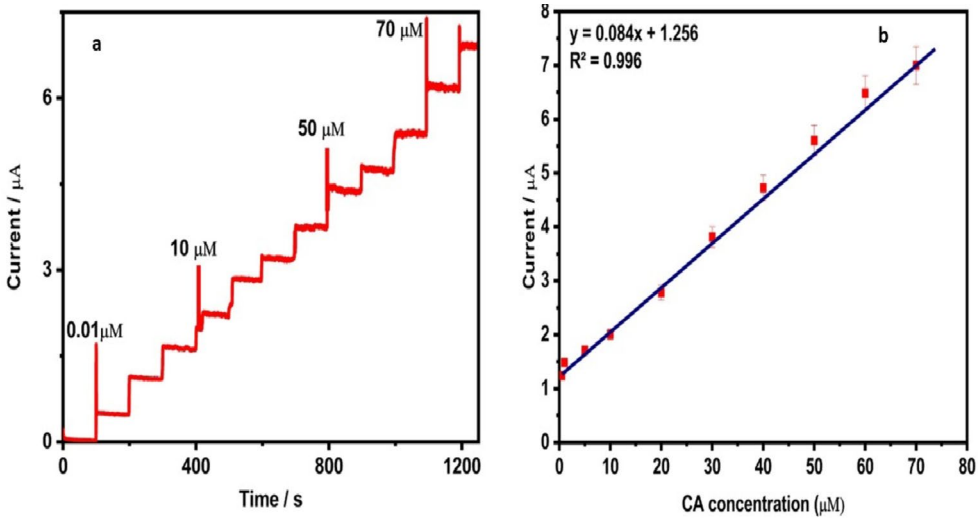

Fig. 7. (**a**) Amperometry i–t curve for CA detection at CaO/g-C_3N_4/PVA modified RDGCE. Each addition increases the concentration of 10μM of CA at 50 s time interval. (**b**) Calibration plot for the linear dependence of peak current vs. concentrations of CA at CaO/g-C_3N_4/PVA modified GCE in 0.1 M PBS (pH 7.0).

Sensing materials	Electrochemical Method	Linear range (μM)	LOD (μM)	Refs.
$CoFeSe_2$/f-CNF/GCE[a]	DPV	1.0-263.96	0.002	42
CdO/SWCNTs/CPE[b]	LSV	0.02–200.0	0.009	16
PGA/GCE	DPV	4.0–30.0	3.91	49
Molecularly imprinted siloxanes modified electrode	DPV	0.5–60.0	0.15	50
Bi_2S_3/CNF/GCE	DPV	0.1–500.0	0.108	39
PdRu/N-SCs/GCE	DPV	0.001–15,000	0.00019	21
$CuZnO_x$/MWCNTs/GCE	DPV	1.0-100.0	0.155	51
BF@rGO-modified electrode	CV & DPV	0.01-892.51	0.00077	20
Au@Co_3O_4@CeO_2/GCE	DPV	0.001–3.0	0.00057	17
MCO/GR/GCE	CV	0.01- 447.19	0.003	15
$CoFeSe_2$/f-CNF/GCE	DPV	-	0.002	41
Au/Pd/GRFE[c]	DPV	0.03-938.97	0.006	34
Ag/$SrFeO_3$/GCE	Chronoamperometry	0.001–0.015	0.023	52
ZnS@RGO/GCE	DPV	0.015–671.7	0.00329	53
ZrO_2/Co_3O_4/RGO[d]/GCE	DPV	0.054–424	0.0013	54
Cu_2S/GOS/SPCE[e]	Amperometry	0.055–2455	0.00022	55
Laccase-MWCNT[f]-CS/ Au	Amperometry	0.7–10	0.150	56
Nafion/GO[g]/GCE	DPV	0.1–1500	0.0091	57
CaO/g-C_3N_4/PVA	Amperometry	0.01 -70.0	0.0024	*Present work

Table 1. Comparison of the CA sensing using various reported electrode materials. [a]GCE-glassy carbon electrode; [b]CPE-carbon paste electrode; [c]GRFE- graphene flakes electrode; [d]RGO-reduced graphene oxide; [e]SPCE-screen printed carbon electrode; [f]MWCNT-multiwalled carbon nanotube; [g]GO-graphene oxide.

PVA modified RDGCE surface. CaO/g-C_3N_4/PVA modified RDGCE determines the CA even at 0.01 μM concentration indicating the rapid diffusion and interaction of CA over the surface of the electrode. The detection limit was calculated using the formula LOD = 3.3 (S/b), where S is the standard deviation and b is the slope of the calibration plot attained from amperometric technique[48]. The proposed electrochemical sensor was exhibited the linearity while increasing the concentration of CA ranges between 0.01 μM and 70.0 μM with correlation coefficient (R^2) value found to be 0.9765 and the calibration plot of peak current against concentration of CA is given in Fig. 7(b). From the calibration plot, the limit of detection (LOD) and sensitivity was calculated to be 0.0024 μM and 11.023 μA μM^{-1} cm^{-2}, respectively. The proposed CA sensor performance was compared with the reported CA sensors are tabulated in Table 1. The electrochemical CA sensor results exhibit an acceptable linear range, excellent sensitivity, and a lower detection limit than other modified electrodes[15–17,20,21,34,39,42,50–52].

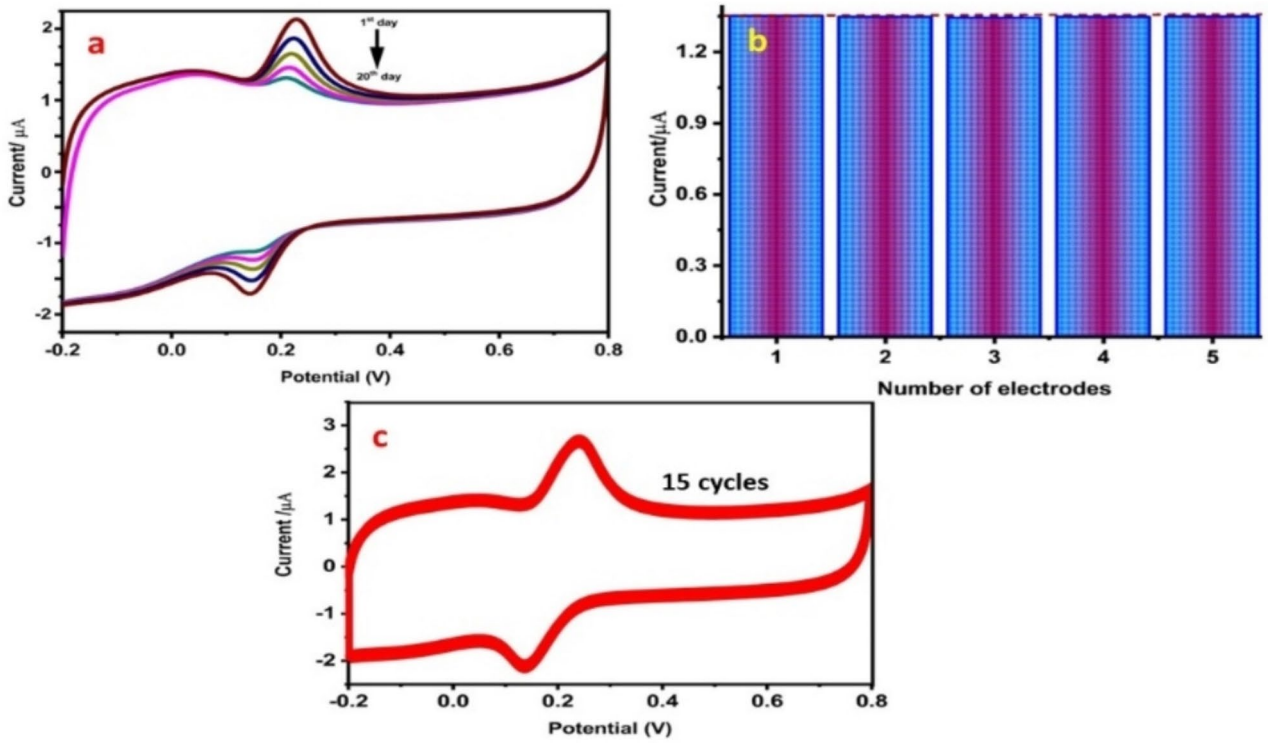

Fig. 8. CV data of (**a**) stability of CaO/g-C_3N_4/PVA modified GCE for the detection of CA for 25 days (5 days interval). (**b**) Reproducibility of the five different CaO/g-C_3N_4/PVA modified GCEs for the detection of CA. (**c**) Repeatability of CaO/g-C_3N_4/PVA modified GCE sensor towards the detection CA assessed by 15-successive measurements in 0.1 M PBS containing 10 µM CA at scan rate 50 mV/s.

Sample	Concentration (µM)		Recovery %	RSD
	Added	Found		
Blood Plasma	25.0	24.5	97.6	1.4
	50.0	49.9	100.1	0.9
	100.0	99.6	99.6	0.5

Table 2. Determination of CA in different blood plasma samples at CaO/g-C_3N_4/PVA modified GCE.

Investigation of stability, reproducibility and repeatability of the sensor

The stability of the CaO/g-C_3N_4/PVA modified GCE was examined for 25 days using 10 µM CA in 0.1 M PBS at pH 7.0 and the oxidation peak current was observed carefully. After 25 days, the peak current was decreased only 1.20% as compared to the peak current obtained of the first day for the detection of CA as shown in Fig. 8a. In addition, the five different successive CV studies towards the detection of CA at 5-different modified electrodes were exhibited the relative standard deviation (RSD) value of 1.78% revealing the CaO/g-C_3N_4/PVA modified GCE hold an admirable reproducibility (Fig. 8b). Repeatability of CaO/g-C_3N_4/PVA modified GCE towards CA was assessed by 15-successive measurements in 10 µM CA under optimized conditions and the RSD value was calculated to be 1.35% supporting the repeatability of CaO/g-C_3N_4/PVA modified GCE (Fig. 8c). The obtained RSD values are good agreement with the reported CA sensor values[14].

Real-time analysis of CA

The practicability of the CaO/g-C_3N_4/PVA modified GCE sensor was applied for the accurate detection of CA in the human blood plasma samples in 0.1 M PBS as a supporting electrolyte at pH 7.0 by cyclic voltammetric technique. The collected human blood plasma samples (25 µM, 50 µM, 100 µM) were dissolved in 0.1 M PBS containing 100 µM of CA by standard addition method. The CA spiked blood plasma samples were examined at CaO/g-C_3N_4/PVA modified GCE sensor by cyclic voltammetric technique. The obtained recovery percentages of the spiked samples are listed in Table 2. The recovery values and RSD values were calculated between 97.6% and 101.1% and 0.5 and 1.4 respectively. The obtained real sample data supports the accurate determination of CA at CaO/g-C_3N_4/PVA/GCE sensor in human blood plasma samples. Under optimized condition, the assay of CA was performed in liquid chromatography coupled mass spectrometry (LC-MS) and the obtained LC-MS

chromatograms of CA standards at three different concentrations (a). 25 µM, (b). 50 µM and (c)0.100 µM in the presence of CaO/g-C_3N_4/PVA nanocomposite in 0.1 M PBS at pH 7.0 and the LC-MS peaks were measured at 1.620 min for all the three different blood plasma sample mixtures at different intensities as given in Fig.S1 along with the detailed procedure.

Conclusion

Calcium oxide nanoparticles (CaO NPs) derived from extract of *Moringa oleifera* leaves decorated graphitic carbon nitride covalently grafted poly vinyl alcohol (CaO/g-C_3N_4/PVA nanocomposite synthesized by sonochemical method and the as-synthesized nanomaterials were characterized by FT-IR, XRD, FE-SEM, EDX and Mapping, TEM, SAED pattern, BET analysis, and electrochemical techniques. Well defined linear range of response and adsorption-diffusion controlled process were confirmed for the redox behavior of CA at CaO/g-C_3N_4/PVA modified GCE in 0.1 M PBS as supporting electrolyte at pH 7.0 under optimized conditions. The Ret value of CaO/g-C_3N_4/PVA modified GCE favors an electron transfer interface between CA and electrode surface. The selectivity of the CaO/g-C_3N_4/PVA modified GCE was confirmed successfully even in the presence of 100-fold excess concentration of interferents for the detection of CA. A suitable two protons and two electrons transfer revisable redox process mechanism was proposed. The LOD and sensitivity values were found to be 0.0024 µM and 11.023 µA μM^{-1} cm^2 by amperometric technique. The stability, repeatability and reproducibility of the proposed sensor were found to be good. The practicability of the proposed sensor was analyzed for CA in blood plasma samples and obtained good recovery results. Furthermore, the proposed method of fabrication of ternary nanocomposite sensor can be used to develop a suitable portable, low-cost device for the selective and accurate detection of CA in food supplements and pharmaceutical fields in future.

Data availability

The data available on request from the corresponding author; periyakaruppankaruppasamy@gmail.com.

Received: 27 August 2024; Accepted: 15 November 2024
Published online: 20 November 2024

References

1. Bounegru, A. V. & Apetrei, C. Voltamperometric Sensors and biosensors based on Carbon nanomaterials used for detecting Caffeic Acid-A Review. *Int. J. Mol. Sci.* **21**, 9275 (2020).
2. Chen, T. W. et al. Sonochemical synthesis of graphene oxide sheets supported Cu_2S nanodots for high-sensitive electrochemical determination of caffeic acid in red wine and soft drinks. *Compos. Part. B Eng.* **158**, 419–427 (2019).
3. Duan, Q., Cao, J. & Zhang, J. Analysis of phenolic acids and their antioxidant activity by capillary electrophoresis-mass spectrometry with field-amplified sample injection. *Anal. Methods*. **4**, 3027 (2012).
4. Razboršek, M. I., Ivanović, M. & Kolar, M. Validated Stability-Indicating GC-MS method for characterization of forced Degradation products of *Trans*-Caffeic Acid and *Trans*-Ferulic Acid. *Molecules* **26**, 2475 (2021).
5. Pereira, F. J., Rodríguez-Cordero, A., López, R., Robles, L. C. & Aller, A. J. Development and validation of an RP-HPLCPDA method for determination of Paracetamol, Caffeine and Tramadol Hydrochloride in Pharmaceutical formulations. *Pharmaceuticals* **14**, 466 (2021).
6. Zhou, W. et al. Simultaneous determination of caffeic acid derivatives by UPLC–MS/MS in rat plasma and its application in pharmacokinetic study after oral administration of *Flos Lonicerae–Fructus Forsythiae* herb combination. *J. Chromatogr. B.* **949–950**, 7–15 (2014).
7. Tanaka, T., Kimura, K., Kan, K., Shindo, T. & Sasamoto, T. Determination of Caffeine, Theobromine, and Theophylline in Chocolate using LC-MS. *F Hyg. Saf. Sci.* **62**, 119–124 (2021).
8. Hsu, B. Y., Lin, S. W., Stephen Inbaraj, B. & Chen, B. H. Simultaneous determination of phenolic acids and flavonoids in Chenopodium Formosanum Koidz. (djulis) by HPLC-DAD-ESI–MS/MS. *J. Pharm. Biomed. Anal.* **132**, 109–116 (2017).
9. Yao, X. & Chen, G. Simultaneous determination of *p*-hydroxyacetophenone, chlorogenic acid, and caffeic acid in Herba Artemisiae Scopariae by capillary electrophoresis with electrochemical detection. *Anal. Bioanal Chem.* **388**, 475–481 (2007).
10. Belay, A. Spectrophotometric Method for the determination of Caffeic Acid Complexation and Thermodynamic properties. *Int. J. Biophys.* **2** (2), 12–17 (2012).
11. Tan, H. et al. A rhodamine 110 loaded and molecularly imprinted polymers coated millipore filter membrane-based fluorescent sensor for sensitive and selective caffeic acid detection. *Microchem J.* **201**, 110588 (2024).
12. Feng, M., Zhang, X. & Huang, Y. Cationic regulation of specificity and activity of defective MCo_2O_4 nanozyme (M = fe, Co, Ni, Cu) for colorimetric detection of caffeic acid. *Talanta* **271**, 125714 (2024).
13. Wang, J. et al. Engineered photoelectrochemical platform for the ultrasensitive detection of caffeic acid based on flower-like MoS_2 and PANI nanotubes nanohybrid. *Sens. Actuators B: Chem.* **276**, 322–330 (2018).
14. Balaji, P. et al. Rapid detection of caffeic acid in food beverages using a non-enzymatic electrochemical sensor based on a Bi_2S_3/CNF nanocomposite. *Sustain. Food Technol.* **2**, 717–728 (2024).
15. Sakthi Priya, T. et al. Non-enzymatic electrochemical detection of caffeic acid in food samples with spinel magnesium cobalt oxide incorporated graphene nanohybrid electrocatalyst. *J. Alloys Compd.* **1002**, 175335 (2024).
16. Arab, Z., Jafarian, S., Karimi-Maleh, H. K., Nasiraie, L. R. & Ahmadi, M. Electrochemical sensing of caffeic acid antioxidant in wine samples using carbon paste electrode amplified with CdO/SWCNTs. *J. Electrochem. Sci. Eng.* **14** (1), 75–82 (2024).
17. Yang, Y. et al. ZIF-derived porous carbon loaded multicomponent heterostructured yolk@shell nanospheres as an ultrasensitive electrochemical sensing platform for the detection of caffeic acid in food. *Electrochim. Acta*. **486**, 144147 (2024).
18. Zheng, L. et al. In situ NH2-MIL-101(fe) Nanoparticles Modified Pencil Core Electrodes for Simultaneous Ratiometric Electrochemical Detection of Caffeic Acid and Acetaminophen. *ACS Appl. Nano Mater.* **Article ASAP** https://doi.org/10.1021/acsanm.4c02317 (2024).
19. Haldorai, Y., Kumar, S., Ramesh, R., Kumar, S. R., Yang, W. & R.T. & Chemical vapor deposition-grown single-layer graphene-supported nanostructured Co_3O_4 composite as binder-free electrode for asymmetric supercapacitor and electrochemical detection of caffeic acid. *J. Alloys Compd.* **995**, 174738 (2024).
20. Catherin Meena, B. et al. Fabrication of M-type barium ferrite ($BaFe_{12}O_{19}$) grafted reduced graphene oxide (BF@rGO) nanocomposite using ethyl imidazolium lactate ionic-liquid: an effective electrode modifier for caffeic acid sensor. *Ceram. Int.* **50** (11), 18708–18717 (2024).

21. Li, Y. et al. An ultrasensitive dietary caffeic acid electrochemical sensor based on Pd-Ru bimetal catalyst doped nano sponge-like carbon. *Food Chem.* **425**, 136484 (2023).
22. Foroughi, M. M., Jahani, S. & Rashidi, S. Simultaneous detection of ascorbic acid, dopamine, acetaminophen and tryptophan using a screen-printed electrode modified with woolen ball-shaped La3+/TiO_2 nanostructure as a quadruplet nanosensor. *Microchem J.* **198**, 110156 (2024).
23. Foroughi, M. M., Jahani, S., Rashidi, S., Tayari, O. & Moradalizadeh, M. The development of electrochemical DNA biosensor based on woolen ball-shaped La^{3+}/TiO_2 nanostructure coating: nanomolar detection of Vinorelbine. *Mater. Chem. Phys.* **315**, 128893 (2024).
24. Mashhadizadeh, M. H., Ghalkhani, M. & Sohouli, E. Synthesis and characterization of N-MPG/CuS flower-like/MXene to modify a screen-printed carbon electrode for electrochemical determination of nalbuphine. *J. Electroanal. Chem.* **957**, 118130 (2024).
25. Saraban, M. et al. A disposable electrochemical caffeine sensor based on a screen-printed electrode modified with a copper-metal organic framework and functionalized multi-walled carbon nanotube nanocomposite. *New. J. Chem.* **48**, 3638–3645 (2024).
26. Manavalan, S., Veerakumar, P., Chen, S. M., Murugan, K. & Lin, K-C. Binder free modification of a glassy carbon electrode by using porous carbon for voltammetric determination of nitro isomers. *ACS Omega*. **4** (5), 8907–8918 (2019).
27. Sriram, B., Gouthaman, S., Wang, S. F. & Hsu, Y. F. Cobalt molybdate hollow spheres decorated graphitic carbon nitride sheets for electrochemical sensing of dimetridazole. *Food Chem.* **430**, 136853 (2024).
28. Kogularasu, S., Sriram, B., Wang, S-F. & Sheu, J-K. Sea Urchin-Like Bi_2S_3 microstructures decorated with Graphitic Carbon Nitride nanosheets for Use in Food Preservation. *ACS Appl. Nano Mater.* **5** (2), 2375–2384 (2022).
29. Sriram, B. et al. Electrochemical sensor-based barium zirconate on sulphur-doped graphitic carbon nitride for the simultaneous determination of nitrofurantoin (antibacterial agent) and nilutamide (anticancer drug). *J. Electroanal. Chem.* **901**, 115782 (2021).
30. Karuppasamy, P. et al. Sonochemical Synthesis and characterization of visible light driven CuO@g-C_3N_4 Nano-Photocatalyst for Eriochrome Black T Dye Degradation in Industrial Dye Effluent. *Russ J. Inorg. Chem.* **67**, 2153–2165 (2022).
31. Karthika, A., Karuppasamy, P., Selvarajan, S., Suganthi, A. & Rajarajan, M. Electrochemical sensing of nicotine using CuWO4 decorated reduced graphene oxide immobilized glassy carbon electrode. *Ultrason. Sonochem*. **55**, 196–206 (2019).
32. Sriram, B., Baby, J. N., George, M., Joseph, X. B. & Tsai, J. T. Surface Engineering of three-dimensional-like hybrid AB_2O_4 (AB = Zn, Co, and Mn) wrapped on sulfur-doped reduced Graphene Oxide: investigation of the role of an Electrocatalyst for Clioquinol Detection. *ACS Appl. Electron. Mater.* **3** (1), 362–372 (2021).
33. Thangavelu, K. et al. Electrochemical determination of Caffeic Acid in Wine samples using reduced Graphene Oxide/Polydopamine Composite. *J. Electrochem. Soc.* **163**, B726–B731 (2016).
34. Thangavelu, K., Raja, N., Chen, S. M. & Liao, W. C. Nanomolar electrochemical detection of caffeic acid infortified wine samples based on gold/palladium nanoparticles decorated graphene flakes. *J. Colloid Interface Sci.* **501**, 77–85 (2017).
35. Ogbonna, C. & Kavaz, D. Green synthesis of hybrids of zinc oxide, titanium oxide, and calcium oxide nanoparticles from Foeniculum vulgare: an assessment of biological activity. *Chem. Eng. Commun.* **211** (7), 1072–1098 (2024).
36. Bounegru, A. V. & Apetrei, C. Voltammetric sensors based on nanomaterials for detection of caffeic acid in food supplements. *Chemosensors* **8** (2), 41 (2020).
37. Naik, T. S. S. K. et al. Green and sustainable synthesis of CaO nanoparticles: its solicitation as a sensor material and electrochemical detection of urea. *Sci. Rep.* **13**, 19995 (2023).
38. Karthika, A., Suganthi, A. & Rajarajan, M. An in-situ synthesis of novel V_2O_5/G-C_3N_4/PVA nanocomposite for enhanced electrocatalytic activity toward sensitive and selective sensing of folic acid in natural samples. *Arab. J. Chem.* **13**, 3639–3652 (2020).
39. EErady, V. et al. Carbon paste modified with Bi decorated multi-walled carbon nanotubes and CTAB as a sensitive voltammetric sensor for the detection of caffeic acid. *Microchem J.* **146**, 73–82 (2019).
40. Botelho, C. N. et al. C.S. Photoelectrochemical-Assisted determination of caffeic acid exploiting a composite based on carbon nanotubes, cadmium telluride quantum dots, and titanium dioxide. *Anal. Methods*. **11**, 4775–4784 (2019).
41. Nehru, R., Hsu, Y. F. & Wang, S. F. Electrochemical determination of caffeic acid in antioxidant beverages samples via a facile synthesis of carbon/iron-based active electrocatalyst. *Anal. Chim. Acta*. **1122**, 76–88 (2020).
42. Sakthivel, M. et al. Entrapment of bimetallic CoFeSe2 nanosphere on functionalized carbon nanofiber for selective and sensitive electrochemical detection of caffeic acid in wine samples. *Anal. Chim. Acta*. **1006**, 22–32 (2018).
43. Vikram, J. et al. Green Synthesized Calcium Oxide nanoparticles (CaO NPs) using leaves Aqueous Extract of *Moringa oleifera* and evaluation of their antibacterial activities. *J. Nanomater.* **2022**, 1–7 (2022).
44. Morsy, M., Gomaa, I., Mokhtar, M. M., ElHaes, H. & Ibrahim, M. Design and implementation of humidity sensor based on carbon nitride modified with graphene quantum dots. *Sci. Rep.* **13** (1), 2891 (2023).
45. Sabarinathan, C., Karuppasamy, P., Vijayakumar, C. T. & Arumuganathan, T. Development of methylene blue removal methodology by adsorption using molecular polyoxometalate: kinetics, thermodynamics and mechanistic study. *Microchem J.* **146**, 315–326 (2019).
46. Zhu, Y., Wu, S. F. & Wang, X. Nano CaO grain characteristics and growth model under calcination. *Chem. Eng. J.* **175** (1), 512–518 (2011).
47. Giacomelli, C., Ckless, K., Galato, D. & Da Silva Miranda, F. Electrochemistry of caffeic acid aqueous solutions with pH 2.0 to 8.5. *J. Braz Chem. Soc.* **13** (3), 332–338 (2002).
48. Kalimuthu, P. & Abraham John, S. Selective electrochemical sensor for folic acid at physiological pH using ultrathin electropolymerized film of functionalized thiadiazole modified glassy carbon electrode. *Biosens. Bioelectron.* **24** (12), 3575–3580 (2009).
49. Santos, D. et al. Application of a glassy Carbon Electrode modified with poly(glutamic acid) in Caffeic Acid determination. *Microchim Acta*. **151**, 127–134 (2005).
50. Leite, F. R. F., Santos, W. D. J. R. & Kubota, L. T. Selective determination of caffeic acid in wines with electrochemical sensor based on molecularly imprinted siloxanes. *Sens. Actuators B: Chem.* **193**, 238–246 (2014).
51. Xie, A. et al. A caffeic acid sensor based on CuZnOx/MWCNTs composite modified electrode. *Microchem J.* **161**, 105786 (2021).
52. Girija, K., Thirumalairajan, S. & Hariharan, V. M. Development of Promising Flower-like Ag/$SrFeO_3$ Nanosheet Electrode materials: an efficient and selective Electrocatalytic detection of Caffeic Acid in Coffee and Green Tea. *ACS Omega*. **8** (49), 46414–46424 (2023).
53. Vinoth, S., Govindasamy, M., Wang, S. F. & Anandaraj, S. Layered nanocomposite of zinc sulfide covered reduced graphene oxide and their implications for electrocatalytic applications. *Ultrasonics- Sonochem*. **64**, 105036 (2020).
54. Puangjan, A. & Chaiyasith, S. An efficient ZrO_2/Co_3O_4/reduced graphene oxide nanocomposite electrochemical sensor for simultaneous determination of gallic acid, caffeic acid and protocatechuic acid natural antioxidants. *Electrochim. Acta*. **211**, 273–288 (2016).
55. Chen, T. W. et al. Sonochemical synthesis of graphene oxide sheets supported Cu2S nanodots for high sensitive electrochemical determination of caffeic acid in red wine and soft drinks. *Compos. B Eng.* **158**, 419–427 (2019).
56. Fulcrand, H., Cheminat, A., Brouillard, R. & Cheynier, V. Characterization of compounds obtained by chemical oxidation of caffeic acid in acidic conditions. *Phytochem* **35**, 499–505 (1994).
57. Filik, H. et al. Square-wave stripping voltammetric determination of caffeic acid on electrochemically reduced graphene oxide–nafion composite film. *Talanta* **116**, 245–250 (2013).

Author contributions

AK, CS & BT; Conceptualization, Data curation, Formal analysis, Investigation, Methodology, SM & KSA: Formal analysis, Visualization; PKS: Writing an original draft, Review & Editing, Supervision; KBT & HCA: Resources, Review & Editing.

Declarations

Competing interests

The authors declare no competing interests.

Ethical approval

Annamalai Karthika, Research Scholar, Department of Chemistry, Thiagarajar College, Kamarajar Salai, Madurai-625 009, India did the experimental research. It is not a field study, but she collected the Moringa oleifera leaves for the purpose of synthesising CaO NPs from inside the college premises not collected from anywhere else.

Additional information

Supplementary Information The online version contains supplementary material available at https://doi.org/10.1038/s41598-024-80146-2.

Correspondence and requests for materials should be addressed to P.K., K.B.T. or H.C.A.M.

Reprints and permissions information is available at www.nature.com/reprints.

Publisher's note Springer Nature remains neutral with regard to jurisdictional claims in published maps and institutional affiliations.